Magnetic field effects on melt convection during crystal growth

Koichi KAKIMOTO and Hiroyuki OZOE

Institute of Advanced Material Study, Kyushu University, 6-1 Kasuga-Koen, Kasuga 816 Japan

Fax +81-92-583-7838, e-mail kakimoto@cm.kyushu-u.ac.jp

Abstract

Oxygen transfer in silicon melts during crystal growth under vertical magnetic fields is investigated numerically and experimentally. A three-dimensional numerical simulation, including melt convection and oxygen transport, is carried out to understand how oxygen transfers in the melt under magnetic fields. Oxygen concentrations in single silicon crystals grown from the melt under these magnetic fields are experimentally measured by using an infrared absorption technique. The results obtained are compared to results from a numerical simulation. An anomalous increase is observed in the oxygen concentration of the grown crystals under a magnetic field of about 0.03 tesla. The cause of this anomaly is identified as Benard instability, since the temperature at the bottom of the crucible is higher than that at interface. When the temperature at the bottom is decreased, the Benard cell can be removed, and a monotonical decrease in the oxygen concentration in the single silicon crystals can be observed.

1. Introduction

Controlling both the absolute value and the fluctuation of the oxygen concentration is crucial to obtain high quality crystals, especially large diameter crystals, since the magnetic field works effectively for melts with large diameters. One way to control oxygen concentration in silicon crystals is to manipulate the fluid flow during crystal growth by using vertical, horizontal and cusp types magnetic fields [1-7]. However, several degrees of freedom also offer several parameters which need to control to make the magnetic fields effective. Therefore, the effects of the magnetic field on the flow pattern and the impurity transfers in the melt should be understood so that we can control these phenomena. There have been several reports that oxygen concentrations in crystals grown monotonically decrease when the horizontal magnetic field increases. The changes in the concentrations reported using vertical magnetic fields are not as simple: they decrease until the magnetic fields reaches about 0.05 tesla, and increase until about 0.1 tesla [8,9]. Finally, they decrease again when the magnetic field is increased continuously. These phenomena can not be explained by the simple idea that the velocity of the melt decreases monotonically when the magnetic fields increases.

The purpose of this paper is to investigate the oxygen transfer mechanism in the melt under vertical magnetic fields by using both a numerical simulation with a three-dimensional configuration and a silicon crystal growth experiment. We focus on the anomaly of oxygen concentration variation under the vertical magnetic field, which can be observed from about 0.05 T to about 0.15 tesla.

2. Experimental

Single silicon crystals with 1.5-inches diameters were grown under vertical magnetic fields from 0 tesla to 0.3 tesla to observe their oxygen concentrations. Details of the growth

furnace can be found elsewhere [10]; we only report on the growth furnace characteristics. Two kinds of heating systems introduced in Figs. 1 (a) and (b) were employed to modify the flow pattern in the melt. The heating system in Fig. 1 (a) makes the temperature distribution at the bottom of the crucible cold, while the system in Fig. 1 (b) makes the temperature at the bottom hot. In this paper, we call the first system type A and the second system type B. All experiments were performed under similar conditions. The experiments were performed with 300g of starting materials within a 3-inch diameter crucible. The crystals were rotated at 3 rpm, and had similar heater power. The rotating rate of the crucible was set at -1 rpm. The pulling rate of the crystals was kept at 1 mm/min. The oxygen concentrations in grown crystals were measured using an infrared absorption method (FTIR) at room temperature.

3. Numerical simulation

Numerical simulation with a three-dimensional configuration with a grid of 60x40x40 in r, θ, z directions was carried out with vertical magnetic fields up to 0.3 tesla. The geometry of the present calculation was set identical to the experimental one with a 3-inch diameter crucible and 1.5-inch crystals. The control volume method was used for discretizing the governing equations such as continuity, Navier-Stokes, energy, and impurity transfer equations in the present calculation. The calculation method for the melt flow has been published in detail elsewhere [11], therefore, in this section we focus on the calculated results. We ignored the electric current through the solid-liquid interface [12,13], although the effect can slightly modify the flow field. The temperature at the bottom of the crucible was set at two different values, 1412° C (melting point) which is identical to type A, and 1430° C, which is identical to type B.

Regarding the calculation of oxygen concentration in the melt, the boundary conditions are imposed as follows. Thermophysical properties are listed in Table 1. The oxygen concentration on a crucible wall should be the value expressed by eq. (1) [14],

$$O = 3.99 \times 10^{23} \exp(-2.0 \times 10^{4} / T) \quad \text{atoms} / \text{cm}^3 \tag{1}$$

where T is absolute temperature. Evaporation of the oxygen through melt-gas interface is taken into account by introducing flux density as shown by eq. (2),

$$q = \text{h(O(melt) - O(gas))} \tag{2}$$

where h, O(melt) and O(gas) are respectively the mass transfer coefficient, oxygen concentration at the surface, and the oxygen concentration in an ambient gas. In the present study, the mass transfer coefficient and the oxygen concentration in an ambient gas were imposed as 1 and 0 atoms/cm^{-3}, respectively. Segregation coefficient of the oxygen concentration at crystal/melt interface was also imposed as 0.85.

An axisymmetric flow pattern was obtained from the numerical simulation with type A heating system within the magnetic field from 0 tesla to 0.3 tesla. However, a non-axisymmetric flow pattern was observed in the simulation with type B heating system as shown in Figs. 2 (a) and (b), which indicate profiles of the velocity and temperature distribution at the top of the melt under a magnetic field of 0.1 tesla. To understand the non-axisymmetric structure in more detail, the velocity profile in z-θ plane is shown in Fig. 2 (c). A cell structure similar to Benard cells can be recognized [15]. This cell structure can be observed only with

the type B heating system, and it was not observed with the type A system. This suggests that the origin of the cell structure was Benard instability. Since vertical magnetic fields were applied to the melt, radial flow was suppressed due to the Lorentz force. Consequently, the temperature gradient of the melt increases and the system becomes unstable because of the cold melt sitting on top of the hot melt. Formation of the Benard cells relaxes the unstable temperature distribution, and the system becomes more stable.

4. Discussion

Calculated oxygen concentrations from the center of the crystals grown from the melt with a height of 3.75 cm are indicated in Fig. 3 (a) by a solid line. The experimental results are indicated by a broken line for type B heating system. The absolute values of the numerical results are slightly different from those of the experimental results. This discrepancy may be due to unknown parameters such as the segregation coefficient, evaporation rate at the free surface, and the dissolution rate at melt-crucible interface used in the present numerical simulation. The anomaly of the oxygen concentration for both the experimental and numerical results was observed at 0.1 tesla. The anomaly was not observed for type A heating system as shown in Fig. 3(b). The solid line indicates calculated results and the broken line indicates experimental results. The anomaly can be attributed to the formation of Benard cells, since the strength of the magnetic field in which the anomaly was observed was almost identical to that in the formation of Benard cells. Oxygen concentration decreased again above magnetic fields because the oxygen diffuses to the top of the melt and evaporates into the gas phase.

5. Conclusion

We studied the oxygen transfer in silicon melts during crystal growth under vertical magnetic field by using a three-dimensional numerical simulation and a silicon crystal growth experiment. The anomalous oxygen concentration increase in grown crystals in a magnetic field of about 0.1 tesla was observed when the temperature at the bottom of the crucible was relatively high. No anomaly was observed when the temperature at the bottom of the crucible was low. The origin of the anomaly was identified as Benard instability. When the Benard cells were formed in the melt, oxygen concentration becomes large. With no cell formation the concentration becomes small.

Acknowledgment

Crystal growth experiment was performed at Fundamental Research Laboratories, NEC Corporation. The author would like to acknowledge Mr. Minoru Eguchi and Dr. Yi Kung-Woo of Fundamental Research Laboratories of NEC Corporation for their skillful experiment and fruitful discussion. A part of this work was conducted as JSPS Research for the Future Program in the Area of Atomic-Scale Surface and Interface Dynamics.

References

[1] H. A. Chedzey and D. T. J. Hurle, Nature **210** (1966) 933.

[2] A. F. Witt, C. J. Herman and H. C. Gatos, J. Mater. Sci. **5** (1970) 882.

[3] K. Hoshi, T. Suzuki, Y. Okuno and N. Isawa, Extended Abstracts of E. C. S. Spring Meeting (The Electrochem. Soc., Pennington, 1981) p. 90.

[4] K. M. Kim, J. Electrochem. Soc. **129** (1982) 427.

[5] R. Moreau, Magnetohydrodynamics, Kluwer academic publishers, (1990).

[6] R. A. Brown, AIChE, **34** (1988) 881.

[5] R. W. Series and D. T. J. Hurle, J. Crystal Growth, **113** (1991) 305.

[6] K. Hoshikawa, Jpn. J. Appl. Phys., **21** (1982) L545.

[7] K. Terashima and T. Fukuda, J. Crystal Growth, **62** (1983) 423.

[8] P. S. Ravishankar, J. Crystal Growth, **104** (1990) 617.

[9] Z. A. Salnick, J. Crystal Growth, **121** (1991) 775.

[10] M. Watanabe, M. Eguchi, K. Kakimoto, H. Ono, S. Kimura and T. Hibiya, **151** (1995) 285.

[11] K.-W. Yi, K. Kakimoto, M. Eguchi, M. Watanabe, T. Syo, and T. Hibiya, **144** (1994) 20.

[12] L. N. Hjellming and J. S. Walker, Int. J. Fluid Mech. **164** (1986) 237.

[13] R. Assaker, N. Van den Bogaert and F. Dupret, J. Magnetohydrodynamics (1995) in press.

[14] H. Hirata and K. Hoshikawa, J. Crystal Growth, **106** (1990) 657.

[15] K. Kakimoto and K.-W. Yi, Physica **B216**, (1996) 406.

Table 1 Thermophysical Properties for numerical Simulation.

Density	Kg/m^3	2520
Heat capacity	J/m^3K	$2.39x10^6$
Dynamic viscosity	Kg/ms	$7x10^{-4}$
Thermal expansion coefficient	K^{-1}	$1.4x10^{-4}$
Latent heat of fusion	J/m^3	$4.14x10^9$
Melting temperature	K	1685
Thermal conductivity	W/mK	45
Emissivity		0.3
Electrical conductivity	S/m	$12.3x10^5$

Figure captions

Fig. 1 Schematic diagram of two kinds of heating system. (a) type A, (b) type B.

Fig. 2 Asymmetric fields of velocity (a) and temperature (b) distribution at the top of the melt. (c) velocity profile in the θ-z plane at the ome-thid of crucible radius.

Fig. 3 Oxygen concentration as a function of magnetic field for type A (a) and type B (b). Solid and broken lines are calculated and experimental results, respectively.

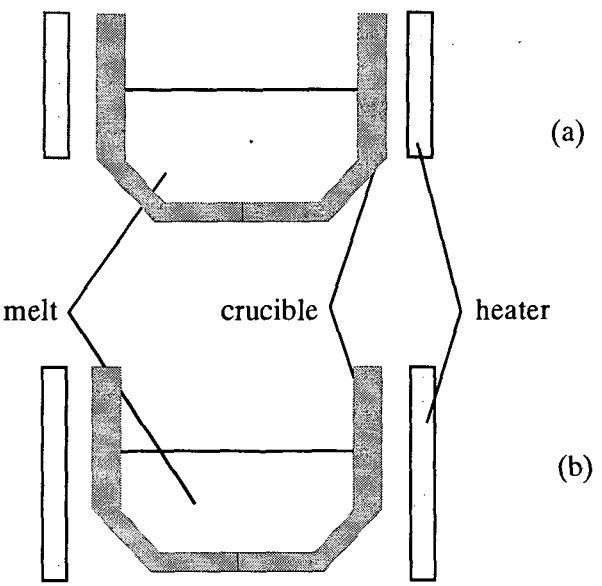

Fig. 1

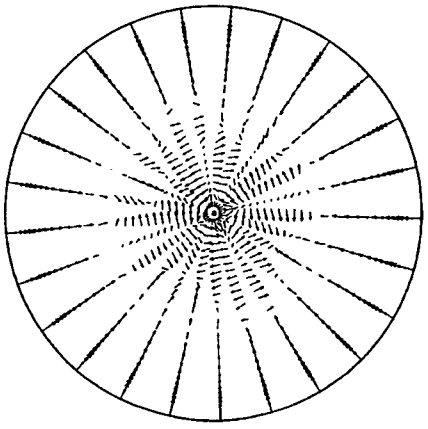

(a)

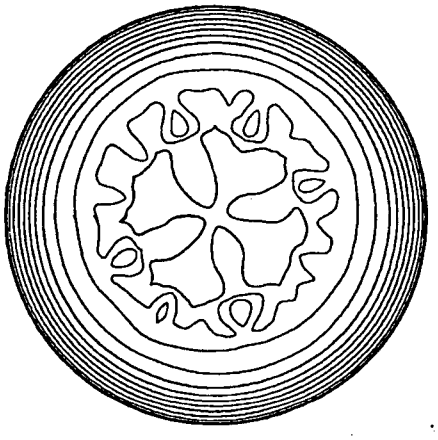

(b)

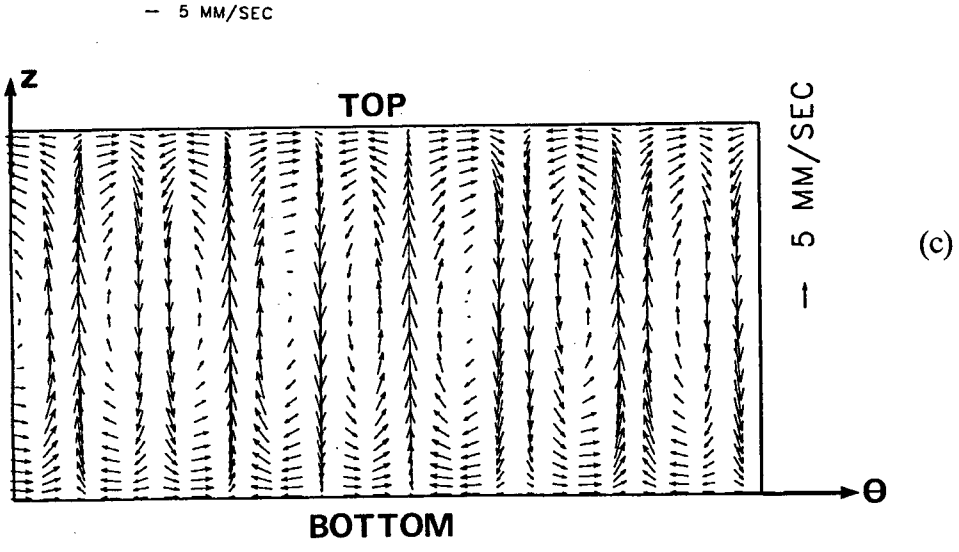

(c)

Fig. 2

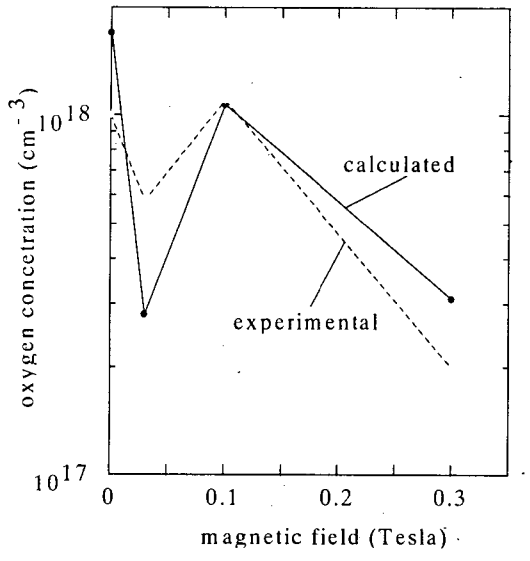
oxygen concetration (cm^{-3})
10^{18}
10^{17}
calculated
experimental
0
0.1
0.2
0.3
magnetic field (Tesla)

(a)

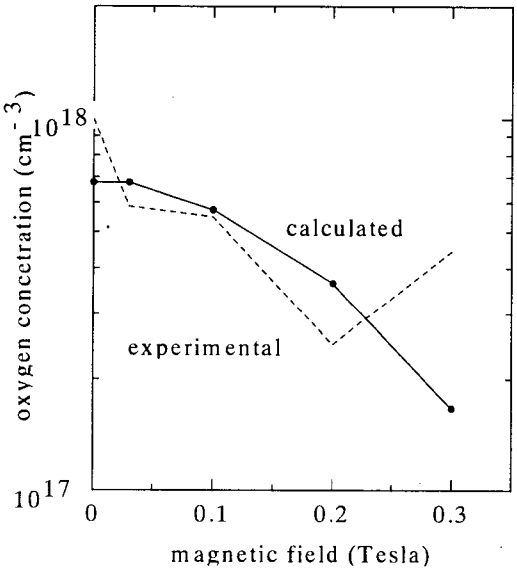
oxygen concetration (cm^{-3})
10^{18}
10^{17}
calculated
experimental
0
0.1
0.2
0.3
magnetic field (Tesla)

(b)

Fig. 3